



# Impact of various Mg(OH)<sub>2</sub> morphologies on hydrophobicity, mechanical, and physical properties of polyurethane nanocomposite

Zahra Rajabimashhadi, Rahim Naghizadeh, Ashkan Zolriasatein, Sonia Bagheri, Claudio Mele, Carola Esposito Corcione

Received: 31 December 2022 / Revised: 16 April 2023 / Accepted: 17 April 2023  
© American Coatings Association 2023

**Abstract** Polyurethane (PU) is one of the best polymer coatings due to its wide range of advantages such as easy fabrication, lightness, non-toxicity, durability, adhesion, flexibility, and strength. However, some of its drawbacks make it a suitable choice for the manufacturing of nanocomposites to enhance its properties. Hydrophobicity and flame retardancy are two of the most crucial characteristics of a polymer nanocoating. Magnesium hydroxide (MH), with its ability to be produced in a multitude of morphologies and exceptional properties, especially in flame retardancy, has always attracted the interest of researchers. One of the best methods for synthesizing high-purity, controlled-size, and controlled-shape nanoparticles is the hydrothermal technique. In this paper, magnesium chloride and sodium hydroxide were utilized as raw materials to synthesize four different morphologies of MH, such as plate, flake, spherical, and disk, functionalized using 3-Aminopropyl triethoxysilane (APTES).

In the following, PU nanocomposites were fabricated by drop casting method including 3 % w.t. of different synthesized MH. The influence of each morphology on different properties of PU/Mg(OH)<sub>2</sub> was then investigated using different analyses such as spectroscopy, mechanical, and hydrophobicity tests. The observations indicated that different surface topography would result from the presence of nanoparticles with various morphologies on the nanocomposite's surface. Extremely high water contact angles were attained as a result of the surface roughness, revealing the super hydrophobic behavior of the produced nanocoatings. Also, the presence of MH in PU matrix improved the mechanical properties of the nanocomposite, depending on the aspect ratio and particle size.

**Keywords** Polyurethane nanocomposite, Magnesium hydroxide, Hardness, Hydrophobicity, Degrading temperature

---

This paper was presented at the 17th Coatings Science International Conference on June 27–30, 2022, in Noordwijk, the Netherlands.

---

Z. Rajabimashhadi, R. Naghizadeh (✉)  
School of Metallurgy and Materials Engineering, Iran  
University of Science and Technology (IUST), Hengam St,  
Narmak, Tehran 16846-13114, Iran  
e-mail: rnaghizadeh@iust.ac.ir

A. Zolriasatein  
Non-metallic Materials Research Department, Niroo  
Research Institute (NRI), End of Dadman St., Tehran  
14686-13113, Iran

S. Bagheri, C. Mele, C. Esposito Corcione (✉)  
Department of Innovation Engineering, University of  
Salento, Edificio La Stecca, via per Monteroni, Lecce 73100,  
Italy  
e-mail: carola.corcione@unisalento.it

## Introduction

Across many different applications, polymer-based coatings are applied to preserve surfaces from destructive agents like solvents, pressure, erosion, wear, corrosion, and other environmental factors.<sup>1,2</sup> Because of their improved bulk properties over pure polymers, polymeric composites have garnered much interest from the scientific community in recent years. As a result, it is currently very appealing to use different reinforcing micro or nanoparticles in polymer matrix composites.<sup>3</sup> Polymers have become increasingly essential among all materials in recent years, whether employed pure or composite, for a variety of applications.<sup>4</sup> Composites are categorized as materials that have defined interfaces or borders among a reinforcement that is microscopically immersed in or adhered to a matrix. The reinforcements aid to improve the

properties of the composite based on the application, and the matrix's role is to hold the reinforcement in the required shapes.<sup>5</sup>

A new and more effective type of composite called polymer nanocomposites is one in which the nanomaterial is completely dispersed throughout the polymeric matrix and has at least one dimension that is on the nanoscale.<sup>6</sup> In particular, applying reinforcement particles to a flexible elastomeric matrix increases strength by adding hard particles and more crosslinking points to the particle-matrix interface. While controlled amounts of ceramic particles with high density, rigidity, fracture toughness, and high thermal stability are mixed with a polymer matrix with weak mechanical properties, low thermal stability, and high flexibility, finally, a nanocomposite with the advantages of both is obtained.<sup>7</sup> Studies in the past found that as the connection between the matrix and the reinforcement improved, the crosslinking of the polymer decreased. In fact, by raising the percentage of reinforcement, two concurrent and conflicting impacts should be taken into account; 1) the favorable influence of increasing the interaction between the reinforcement and the matrix, and 2) the unfavorable influence of decreasing the degree of crosslinking in the polymer.<sup>8,9</sup> On the other hand, homogeneity in this two-component blend could have a significant emphasis on improvement of properties in polymer composites. It is quite evident that when reinforcement is improperly mixed with the matrix, the particles are not well dispersed in the polymer and there is insufficient interaction between them. These aforementioned drawbacks might lead to excessive weaknesses in almost all characteristics of the nanocomposite.<sup>10,11</sup>

Among some of the polymers that have improved via inorganic nanoreinforcement are polypropylene, epoxy, polyamide, polyvinyl chloride, polystyrene, styrene-butadiene rubber, silicone rubber, and polyurethane (PU). PU is an important class of polymer coatings due to its several benefits, including low density, biocompatible and biostable nature, non-toxicity, non-flammability, glossiness, transparency, abrasion resistant nature, great adhesion, durability against weather, anti-aging ability, processability, shape memory, flexibility even in low temperature, high elongation at break, high impact strength, elasticity, and attainable hardness.<sup>9,10</sup> Albeit there are some major drawbacks associated with PU, especially in high-temperature working environments, such as insufficient tensile strength, low thermal stability, poor thermal and electrical conductivity, and low anti-corrosive properties. PU is highly flammable in these conditions and has poor adhesion to metal surfaces. These weaknesses could play roles as barriers to different PU applications. The limitations have led to the fabrication of nanocomposite to recompense for the disadvantages of PU via addition of various reinforcements.<sup>12–14</sup>

PU composites are a widely used material due to their ability to combine the toughness and strength of

metal with the flexibility of rubber. On the other hand, elastomeric PU is routinely enhanced with inorganic reinforcements and is rarely used as a pure polymer.<sup>10,13</sup> Despite the inherent features of PU, there is an ongoing necessity to improve the desirable properties that can be adjusted to satisfy the wide range of needs. For example, in terms of environmental issues, it is critical that PU has a hydrophobic property for prospective application in coatings, hence attempts have been undertaken to improve hydrophobicity.<sup>15,16</sup> PU composites contain block copolymers that have intrinsically great physical properties due to the presence of hard-soft segments in micro phase. Diisocyanate and chain extenders that build the urethane groups are included in a hard segment, whereas polyether or polyester polyol make a soft segment.<sup>15,17,18</sup> Due to the existence of hard segment content, such polymer materials may exhibit characteristics of high glass transition temperature and melting temperature. The final composite qualities depend on the chemical composition, molecular weight, and morphology of PU.<sup>7,19</sup>

A wide range of nano reinforcements has been performed in the scope of nanotechnology to fabricate PU nanocomposites. PU structure may be modified by the application of nano-additives in the matrix. The resistance to corrosive chemicals, moisture, heat, and environmental repellency depends on the increased surface qualities of PU nanocomposite.<sup>20–22</sup> To enhance mechanical, electrical, thermal, surface, and rheological properties, nanomaterials such as TiO<sub>2</sub>, SiO<sub>2</sub>, CaCO<sub>3</sub>, ZnO, and Al<sub>2</sub>O<sub>3</sub> have been used.<sup>23–27</sup> In contrast to conventional micropowders, nanoparticles have a greater surface area, a higher surface energy, and a tendency to aggregate. Surface modification has therefore been viewed as a key solution in numerous investigations. Silane and fluorine materials have been the subject of the majority of studies. However, using these materials for alteration is costly and harmful to both the environment and people's health.<sup>28–30</sup>

Wang et al. have investigated the anti-aging properties of PU/ZnO nanocomposite by SEM and FTIR analysis. They demonstrated that after accelerated aging for 500 h, a sample with 1 % w.t. reinforcement could preserve a better morphological structure than one with 5% w.t.<sup>31</sup> El Saeed et al. also used this nanoparticle in PU composite to evaluate corrosion performance, mechanical and physical properties. They dispersed different amounts of ZnO from 0.1 to 2.0 % w.t. in PU matrix by ultrasonic method. After 500 h of exposure to salt spray tests, PU/ZnO samples were tested against Gram-negative and Gram-positive bacteria for antimicrobial activity evaluation. Results revealed that the growth of organisms on the sample surface was found to slow down. Also, the degree of blistering and percentage of the rusted zone were significantly decreased.<sup>32</sup> Bui et al. have studied the mechanical properties of PU/SiO<sub>2</sub> in different amounts of reinforcement such as 0, 1, 2.5, 5, 7.5, and 10% w.t. The mechanical analysis showed that sample with 2.5%

w.t. is the best one.<sup>33</sup> Also, Song et al. have investigated this nanocomposite. The results revealed that wear resistance of PU was improved via addition of nano SiO<sub>2</sub> due to fine dispersion and interfacial adhesion from 250 to 800 m/μm in 1 and 3% w.t., respectively.<sup>34</sup> According to another study that was performed by Nguyen et al. on PU/TiO<sub>2</sub>, the mechanical analysis indicated that the appropriate amount of nanoparticles was 2% w.t.<sup>35</sup> PU/TiO<sub>2</sub> nanocomposite was also studied by Sabzi et al. Amino propyl trimethoxy silane (APS) was applied for nanoparticle modification to have a better interaction between matrix and reinforcement. Finally, the best sample with 3 % w.t. nanoparticle improved tensile strength by more than 70% and Young's modulus by almost 50%. The proposed mechanism in this paper was the formation of surface interaction between PU/TiO<sub>2</sub>.<sup>36</sup>

Among all studies, investigating magnesium hydroxide (MH) as a fire-resistant, insulating substance and antibacterial agent in nanocomposites is extremely infrequent. One of the most extraordinary aspects is the ability to synthesize MH with various morphologies. Due to the fact that reinforcements in the polymer matrix with varying morphologies might alter characteristics of nanocomposites like hydrophobicity, we used the hydrothermal method to synthesize MH nanoparticles. Hydrothermal synthesis is a method for crystallizing materials that involves chemical reactions in aqueous solutions under pressure and at a temperature above the boiling point. The main advantages of hydrothermally synthesized powders are the low degree of agglomeration and perfect control of crystallite size and morphology by applying different surfactant.<sup>37–41</sup>

To our surprise, we could not find any research on PU/Mg(OH)<sub>2</sub> nanocomposites despite their outstanding potential to synthesize in different morphologies, fire retardancy, antibacterial properties, and so on. The absence of literature and our hypothesis (as described above) encourages us to do the present study, with the main objective to investigate the effect of different morphologies of MH on the hydrophobic, thermal, physical and mechanical properties of PU nanocomposites. In this regard, MH was synthesized from NaOH and MgCl<sub>2</sub> by hydrothermal method (180°C-180 h). Also, four surfactants (1% w.t.) including CTAB, PEG500, gelatin, and oleic acid were used to achieve different morphologies. After MH modification by APTES to obtain fine dispersion in PU matrix, nano-functionalized MH was examined with XRD, FTIR, FESEM, EDS, and DLS. According to the literature review, it is difficult to achieve the favorable properties of polymer-reinforcement at high amounts of filler, and most researchers have reported the optimal percentage to be below 5% w.t. Therefore, we fabricated PU/Mg(OH)<sub>2</sub> nanocomposite following drop casting method with addition of 3% w.t. reinforcement. Finally, the influence of each morphology on different properties was investigated using FESEM,

DSC, AFM, hardness, tensile strength, and contact angle tests.

The rest of the paper is organized as follows: “**Experimental methods and materials**” section includes raw material, synthesis method, sample preparing and analyzing tests in detail. “**Results and discussion**” section includes presentation of characterization and tests performed. Ultimately, we present the paper's conclusion in “**Conclusions**” section.

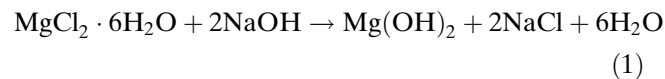
## Experimental methods and materials

The outstanding properties of PU made it well-suited for resistance coatings. However, it suffers from some low physical and mechanical properties, including hydrophobicity, hardness, tensile strength, and thermal stability. To tackle the above-mentioned issues, we exploit the advantages of MH in this study. Its ability to be synthesized with different morphologies is the rationale behind the main idea of our research. The primary contribution of the proposed study is addition of MH with different morphologies to the PU/Mg(OH)<sub>2</sub> nanocomposite. In this regard, we proposed investigating the morphology's impact on the surface properties of nanocomposite (i.e., contact angle). In addition to hydrophobicity, we evaluated the influence of MH on other PU properties such as hardness, tensile strength as well as degrading temperature.

In the following, we present the materials and methods including raw material, composite fabricating process, and analyzing tests in detail.

### Nano-MH synthesis

First, MH with four different morphologies was synthesized by using four different surfactant. All of the materials that were used in this step are listed in Table 1. MH synthesis began by making 1 M magnesium precursor solution (Sol.1) and 2 M sodium hydroxide solution (Sol.2) in distilled water. equation (1) was used to complete the synthesis:



Additionally, Sol.1 was given a 1 % w.t. addition of surfactant, and it was homogenized using magnetic stirring for a total of 10 min. Then, using a glass pipette and a controlled rate of 2 mL/min, Sol.2 was added to Sol.1 and mixed for 10 min on a magnetic stirrer (Sol.3). After that, Sol.3 was soaked in an ultrasonic bath (power: 400 W) for 30 min to make sure the particles were homogeneously dispersed in the solution (Sol.4). The next step was to transfer Sol.4 to a vial glass and put it in an autoclave made of steel and lined with Teflon. Finally, the hydrothermal technique was

**Table 1: Materials used for MH synthesis**

Material	Chemical formula	Role	Manufacture (CAS No.)
Magnesium chloride	MgCl <sub>2</sub> · 6H <sub>2</sub> O	Mg source	Dr. Mojallali (7791-18-6)
Sodium hydroxide	NaOH	Precipitating agent	Dr. Mojallali (1310-73-2)
CTAB	C <sub>19</sub> H <sub>42</sub> BrN	Surfactant	SIGMA (57-09-0)
PEG500	C <sub>24</sub> H <sub>50</sub> O <sub>12</sub>	Surfactant	Merck (24991-55-7)
Gelatin	C <sub>102</sub> H <sub>151</sub> N <sub>31</sub> O <sub>39</sub>	Surfactant	SIGMA (9000-70-8)
Oleic acid	C <sub>18</sub> H <sub>34</sub> O <sub>2</sub>	Surfactant	Merck (112-80-1)
APTES	C <sub>9</sub> H <sub>23</sub> NO <sub>3</sub> Si	Functionalize agent	SIGMA (919-30-2)
Distilled water	H <sub>2</sub> O	Solvent	Ghatran Shimi (7732-18-5)
Ethanol	C <sub>2</sub> H <sub>5</sub> OH	Solvent	Dr. Mojallali (64-17-5)
Isopropyl alcohol	C <sub>3</sub> H <sub>8</sub> O	Solvent	Dr. Mojallali (67-63-0)

used to synthesis MH at 180 °C for 18 h (Sol. 5). The final solution was centrifuged at 5000 rpm for 4 min on each cycle with distilled water and ethanol, three cycles for each one, to get rid of any byproducts or unreacted products. Subsequently, the washed solution was heated in an oven at 120 °C for 5 h to get the synthesized MH powder, which is then prepared for characterization analyses. The synthesis process of nano MH powder is shown in Fig. 1.

### PU/Mg(OH)<sub>2</sub> fabrication

Synthesized MH powder was functionalized by APTES to obtain fine dispersion in PU matrix. In this regard, MH-solution was made in 50 mL of isopropyl alcohol and stirred with a magnetic stirrer at 400 rpm at 80 °C. Then, APTES was gradually added to the stirring mixture in a ratio of MH/APTES=2. After 1 h, the particles were washed using a centrifuge and dried for 5 h at 120 °C. Then, nanoparticles were dispersed in xylene (solvent), mixed for 10 min on magnet stirrer (Sol.6), and ultrasound for 30 min (Sol.7). The resulting solution was added to polyacrylate (resin) and blended. Again, ultrasonic bath was used to obtain a homogeneous mixture. After 30 min, polyisocyanate (hardener) was smoothly added into the solution (Sol. 8). In order to avoid the formation of bubbles in the solution, in the last two steps, mixing was done with a glass stirrer and by hand. Finally, the prepared mixture was slowly poured into a 10 × 10 cm PTFT mold (drop casting method). The curing process was completed after 1 h heating at 90 °C. These steps are entirely shown in Fig. 2 and raw material used in production of PU/Mg(OH)<sub>2</sub> nanocomposite are reported in Table 2.

The chemical information of the samples is listed in Table 3. Density is obtained through the rule of mixtures with specified weight percent and density of components in the final nanocomposite [equation (2)]. According to past references, the ratio of NCO:OH that comes from the ratio of polyacrylate (resin) to polyisocyanate (hardener) was considered 1:2 to obtain

the best qualification of polymer.<sup>42</sup> Then, according to the mold volume, the amount of each component was calculated to obtain a free film with a thickness of 1 cm [equations (3) and (4)].

$$D_{\text{Nanocomposite}} = \left( \frac{X_{\text{MH}}}{D_{\text{MH}}} + \frac{X_{\text{resin}}}{D_{\text{resin}}} + \frac{X_{\text{hardener}}}{D_{\text{hardener}}} \right)^{-1} \quad (2)$$

$$M_{\text{Nanocomposite}} = D_{\text{Nanocomposite}} \times V_{\text{mold}} \quad (3)$$

$$M_{\text{Component}} = X_{\text{Component}} \times M_{\text{Nanocomposite}} \quad (4)$$

Where *D*, *X*, *M*, and *V* indicate density, weight percent, molecular weight, and volume, respectively.

### Characterization

#### Nano-MH powder analysis

In order to evaluate the synthesized nanopowders, X-ray diffraction (XRD), field emission scanning electron microscopy analysis (FESEM), dynamic light scattering (DLS), and Fourier-transform infrared spectroscopy (FTIR) were performed. To evaluate the purity of the synthesis and characterize the structure of MH powder, XRD was used. This test is performed with BOUREVSTNIK DRON-8 X-ray diffraction device equipped with CuK $\alpha$  monofilament with a wavelength of 0.154 nm, an accelerator voltage of 40 kV, and a current of 30 mA and in the range of 10° to 80° angles with steps and 0.5° and stop time of 1 sec per step at 25 °C and one atmospheric pressure with a copper anode. FESEM analysis was used to study the morphology of nanoparticles. FESEM analysis was undertaken using SEM (MIRA3TESCAN-XMU) in high vacuum mode. The radiation source was an Uvc (w5) pencil lamp made by Hach Company, USA. All images were captured at 50000 × magnification with resolution of 1 nm. MH powder solution was made in 5 mL 2-propanol and placed in an ultrasonic bath for 5 min to achieve

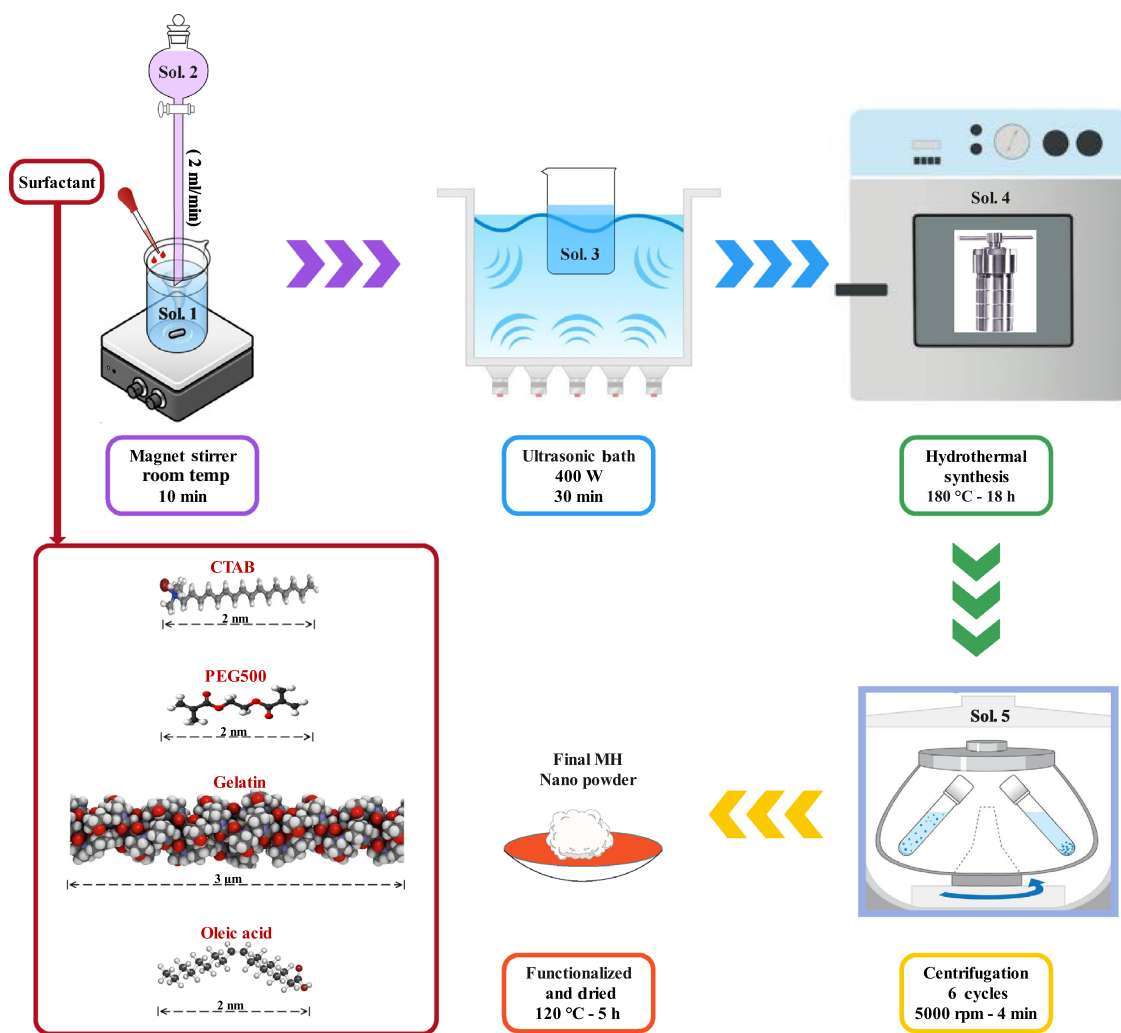


Fig. 1: Synthesis and functionalization of nano MH powder

proper dispersion of the nanoparticles in the solvent and to prevent agglomeration. Then a drop of it was dropped on a glass slide and left to air dry. Due to the insulation of the powder, the gold was coated using the Nano-structure COATING DSR model. DLS analysis was performed to investigate the particle size distribution of the synthesized powders by a non-invasive quantitative technique with the Zetasizer Advance Pro device made in United Kingdom. FTIR spectroscopy was used to evaluate chemical groups of hydrophobic agents on the surfaces of MH nanoparticles with different morphologies.

#### *PU/Mg(OH)<sub>2</sub> nanocomposite analysis*

In order to investigate the effect of nano-MH on different properties of PU/Mg(OH)<sub>2</sub> nanocomposite, field emission scanning electron microscopy analysis (FESEM), differential scanning calorimetry (DSC), atomic force microscopy analysis (AFM), hydropho-

bicity and mechanical tests (hardness and tensile strength) were performed. FESEM analysis was used to study microstructural features, and distribution of MH in composites at 500 × and 5000 × magnification. DSC analysis was carried out to investigate the effect of different morphologies of MH on thermal stability and degrading temperature of nanocomposites. AFM was performed at a 5 × 5-micron cross-sectional area. These represent the surface roughness at the nanometer scale to investigate the function of MH particles in surface topography. Measuring static contact angle was done to study the effect of different morphologies of MH on hydrophobicity of nanocomposite. Type A Durometer (Teclock GS-709 N) was used to measure and compare the hardness of the nanocomposites according to ISO868 standard. This is a device for measuring the hardness of a material, typically of polymers, elastomers, and rubbers. Higher numbers on the scale (Shore A) indicate a more excellent resistance to indentation and thus harder materials. The stress-strain curve for a material gives the relationship

between stress and strain. It is obtained by gradually applying load to a test zone and measuring the deformation, from which the stress and strain can be calculated. This test was executed according to ISO 37 standard on dumbbell-shaped samples with a length of 50 mm and using a tensile testing machine with a gage length of 20 mm and strain rate of 10 mm/min.

## Results and discussion

### Nano-MH powder characterization

In accordance with the JCPDS 7-0239 standard card, all diffraction peaks in Fig. 3 belonged to hexagonal  $Mg(OH)_2$  with lattice constants of  $a = 3.1444\text{\AA}$  and  $c = 4.777\text{\AA}$ . The crystal planes (001), (100), (101), (102), (110), (111), (103), (201), and (201) are identified at diffraction angles of 18.45, 33.24, 37.67, 51.12, 58.78, 62.34, 67.86, 72.15, and 82.22 degrees, respectively. The presence of sharp peaks in the XRD pattern, as well as

the absence of any impurity peaks, further demonstrated that a high-purity single phase of nano-MH was crystallized.<sup>43</sup>

The orientation of MH particles is indicated by the intensity of diffraction in planes (001) and (110). The preferred orientation of hexagonal  $Mg(OH)_2$  is typically in the direction of the plane (001), and this orientation increases as the intensity of the plates (001) and (110) rises. Also, according to the standard card, the (101) intensity should be more than (001). Otherwise, plane (001) is the preferred orientation. As a result, the morphology of the MH-C and MH-P were more uniform in both directions (001) and (101) than MH. In MH-G, however, relatively wide, low-intensity peaks represent finer, spherical particles (similar to the standard phase). In contrast, the sharp and high peaks of the MH-O in both (001) and (101) planes are evidence of its elliptical morphology.<sup>44</sup>

Furthermore, FESEM was used at 50000 × magnification to study the determination of the size and morphology of nanoparticles and EDS analysis was also performed to investigate the elemental composi-

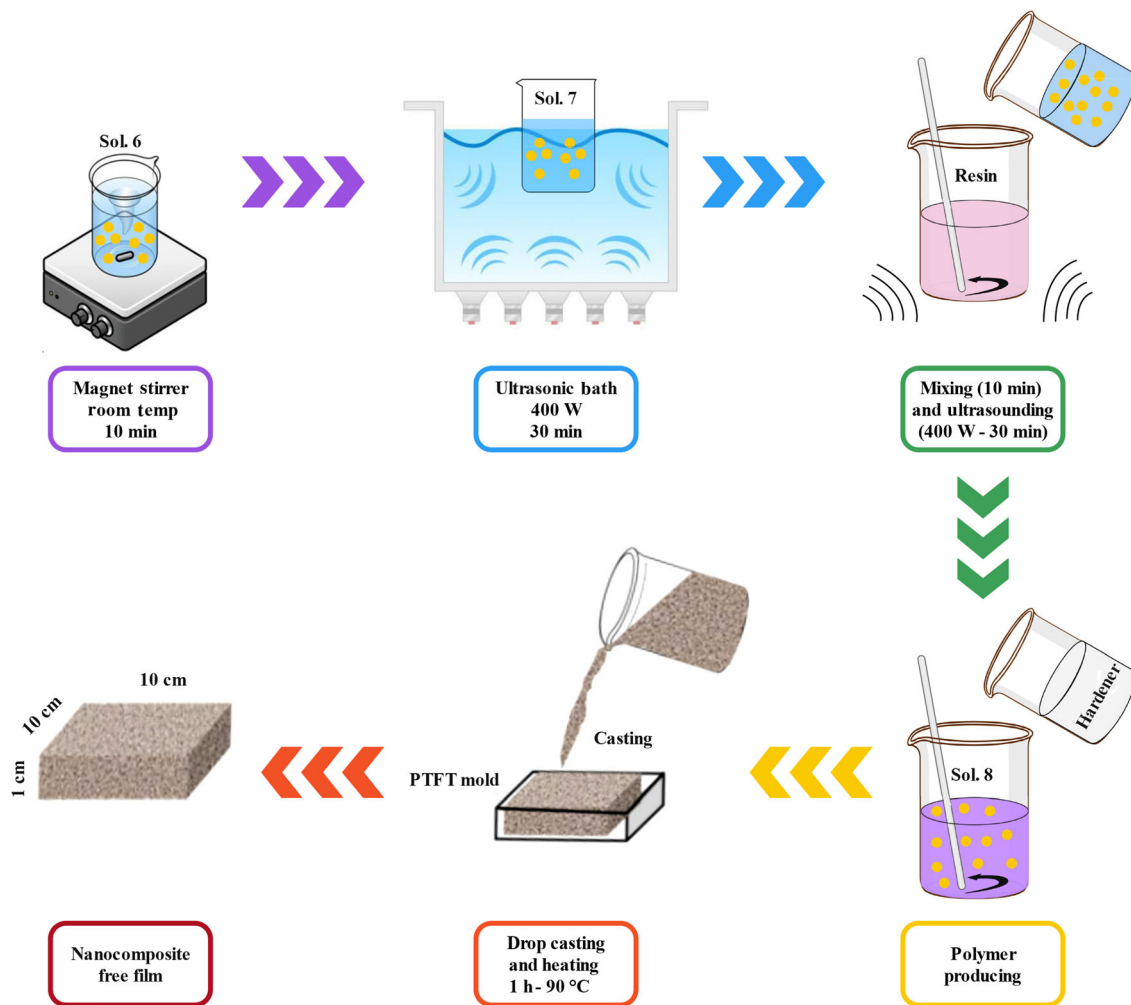


Fig. 2: Production of PU/Mg(OH)<sub>2</sub> nanocomposite

**Table 2: Materials used for PU/Mg(OH)<sub>2</sub> fabrication**

Material	Chemical formula	Manufacture (CAS No.)
Magnesium hydroxide	Mg(OH) <sub>2</sub>	Synthesized
Magnesium hydroxide	Mg(OH) <sub>2</sub> /Flake	Synthesized
Magnesium hydroxide	Mg(OH) <sub>2</sub> / Plate	Synthesized
Magnesium hydroxide	Mg(OH) <sub>2</sub> / Spherical	Synthesized
Magnesium hydroxide	Mg(OH) <sub>2</sub> / Disk	Synthesized
Polyacrylate	Tacryl765X	Taak Resin Kaveh
Polyisocyanate	Desmodur N75	Covestro AG
Xylene	C <sub>8</sub> H <sub>10</sub>	Dr. Mojallali (1330-02-07)

**Table 3: The chemical information of the PU/Mg(OH)<sub>2</sub> nanocomposites**

Component	Role	Weigh percent (% w.t.)	Density (g.cm <sup>-3</sup> )
MH	Reinforcement	3	2.34
Polyacrylate	Resin	65	1
Polyisocyanate	Hardener	32	1.06
Xylene	Solvent	30 (Extra)	–

tion of the samples. EDS images demonstrated the presence of Mg, O, and Au elements in all MH powders. Microstructure characterization was accomplished by an ultrasound solution of nano-MH in 2-propanol. Then, a drop of it was scattered on a glass slide and dried at room temperature. The gold coating was also applied because of the powder's insulation.

The inclusion of surfactant in the synthesis process has a significant impact on product morphology, particle size, and agglomeration, as seen in Fig. 4. In MH synthesis, although the precursor solutions were applied drop wise at an appropriate rate of 5 mL/min in order to obtain pure nano-MH with average diameters below 100 nm, the phenomenon of aggregation and particle clumping occurred due to the lack of surfactant, as seen in the MH-powder FESEM image.<sup>39</sup> The extraordinarily small size of the MH-G sample is observable in the FESEM image of this sample, which is explained by the gelatin chain being long as a surfactant compared to other surfactants. Considering the presence of gelatin in the solution during synthesis, the first crystals could not be overgrown, resulting in overmuch fine nanoparticles with spherical morphology. Another important point is the vertical orientation of MH-P nano-plates, which is expected to have a significant impact on the surface properties of nanocomposites. MH-C is randomly distributed and MH-O is distributed horizontally. However, we have discussed the mechanism of using different surfactants on MH morphology by hydrothermal method in detail in another study.<sup>45</sup>

In the following, DLS analysis was carried out to observe the impact of applying four different surfac-

tants on the particle size and particle size distribution of nano-MH powders. The particle size distribution and diameter in different volumes of particles are shown in Figs. 5 and 6, respectively.

According to Fig. 5, DLS analysis of all samples shows a single-peak diagram providing very fine nanoparticles (10–30 nm) and medium nanoparticles (40–100 nm). Using CTAB in the MC-C sample, a uniform and relatively sharp curve is obtained, which indicates a wide distribution of particle sizes between 60 and 100 nm. However, by adding PEG as a surfactant, a sharper curve was obtained for the MC-P sample, indicating a narrow particle size distribution between 80 and 90 nm. In the case of the MC-G, when adding gelatin with a huge molecule structure, very fine particles were synthesized in the range of 30 to 45 nm, causing the curve to shift to the left and to turn keener. The presence of oleic acid, on the other hand, has resulted in a bigger nano-disk with an average diameter of 90 nm and a relatively wide range of 75–105 nm.<sup>46,47</sup>

In PU coatings, there are two different factors that control the thermal degradation: vibrations and rotations of polymer chains. Small molecules are created as a result of bond dissociation as the temperature rises. The following contains crosslinking, chain-end parts, random chain scissions, and combinations of these pathways. The temperature of the degradation increases as these steps involved occur more prolonged and the thermal stability of polymer improves as well. Indeed, changing the heat release rate is the main mechanism for changing the degradation temperature via addition of nanofillers. A common technique for

influencing the mobility of polymer chains is the addition of nanoparticles. PU thermal stability improvement tends to depend on different parameters of nanofillers such as size, shape, type, amount, and dispersion, as well as filler-matrix interaction. The high surface area of nanofillers would have an effect on interfacial interaction increment and reduce the heat release rate of the polymers. Therefore, high thermal stability could be obtained by applying modified inorganic nanofillers that are uniformly dispersed throughout the organic matrix and interact strongly with it.<sup>48,49</sup>

The FTIR spectra of nano-MH powders after modification by APTES are shown in Fig. 7. The peak at  $3698\text{ cm}^{-1}$ , which is identified in all samples, refers to the -OH bond in  $\text{Mg}(\text{OH})_2$  structure. The peaks that are observed at about  $1620\text{ cm}^{-1}$  in the FTIR spectrum correspond to the stretching mode of C-N and H-N-H as well as the wide peaks around  $1050\text{ cm}^{-1}$ , which belong to the stretching vibration of the Si-O-Si or Si-O-C bonds. These two peaks confirm that the presence of long-chain silane groups on the MH surface come from APTES as a functionalized agent.<sup>50,51</sup> In the end, according to the characterization performed on magnesium powders, some properties of different samples are summarized in Table 4.

### PU/Mg(OH)<sub>2</sub> nanocomposite

#### Microstructure characterization

**FESEM.** Figure 8 compare the surface microstructure of nanocomposite samples with pure polyurethane at

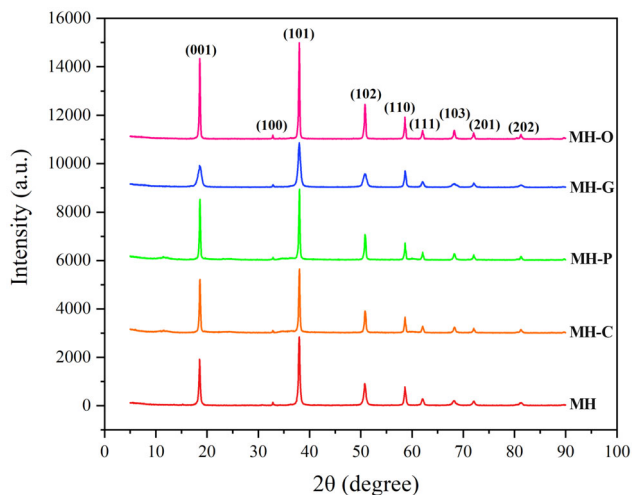


**Fig. 3: X-ray diffraction pattern comparison of MH powders in accordance with the JCPDS 7-0239 standard card. All peaks related to hexagonal  $\text{Mg}(\text{OH})_2$  were identified in samples and according to the intensity of diffraction in a specific crystal plane, the orientation and growth direction of MH crystals were discussed**

$5000\times$  magnification. As demonstrated, the composite samples have a rough surface; the involvement of MH nanoparticles causes this surface roughness, which is one of the significant parameters to improve the hydrophobicity.<sup>41</sup> However, looking at the FESEM images in greater detail, the impact of more factors is discovered including the size, shape, amount, and dispersion of nanoparticles in PU matrix.<sup>1,3</sup> Since each composite studied in this investigation contains 3% w.t. of filler, the effect of the amount can be ignored. It is notable that the surface of PU-G has a less rough texture by comparing the surface micrographs of nanocomposites with different shapes. This consequence can be attributed to the extremely fine size of MH-G nanoparticles as opposed to other synthesized powders (near 40 nm). Moreover, the sphericity of MH-G nanoparticles and the aspect ratio of nearly 1 also had an obvious effect in creating this relatively smooth surface. Nanocoatings are usually applied with a thickness below  $100\text{ }\mu\text{m}$  on the substrate. However, it should be highlighted that nanoparticles have high surface energy, which causes their propensity to aggregate. If nanoparticles agglomerate, the surface roughness of PU nanocoating will be almost unaffected by the different morphology of nanofiller. Therefore, the dispersion of nanoparticles in the polymer matrix is of great importance. For this reason, in addition to surface modification with APTES and applying the hydrophobic agent to nanoparticles, a low filler percentage was applied to the PU matrix (3% w.t.). In these conditions, most of the nanoparticles come to the external surface of the coating due to the difference in density and create different topographies.<sup>52,53</sup>

As the shape of the particles goes out of the spherical state, the aspect ratio moves away from the value of 1. Now these non-spherical MH nanoparticles are able to create surfaces with different roughnesses.<sup>27</sup> With the same reasoning, coarse 90 nm MH-O nanoparticles have created a rougher surface in the PU-O composite. PU-C and PU-P nanocomposites with particle sizes of 79 and 75 nm are not an exception to this norm; the difference is that the distribution and orientation of MH-P on the surface of the nanocomposite is completely evident in the microstructure. Indeed, the rougher surface of PU-C than PU-P cannot be attributed only to the small size difference between MH-C and MH-P (less than 5 nm). In fact, the particles which are evidenced in Fig. 8 are not nanofillers. But these parts refer to the roughness that was caused due to nanofillers presence.

#### Thermal stability

**DSC.** Thermal stability is a crucial property of any material for application purposes, especially when taking into account the potential ultimate uses in various industries. The special temperature or temperature/time range through which a material could be employed without suffering a significant loss of qual-



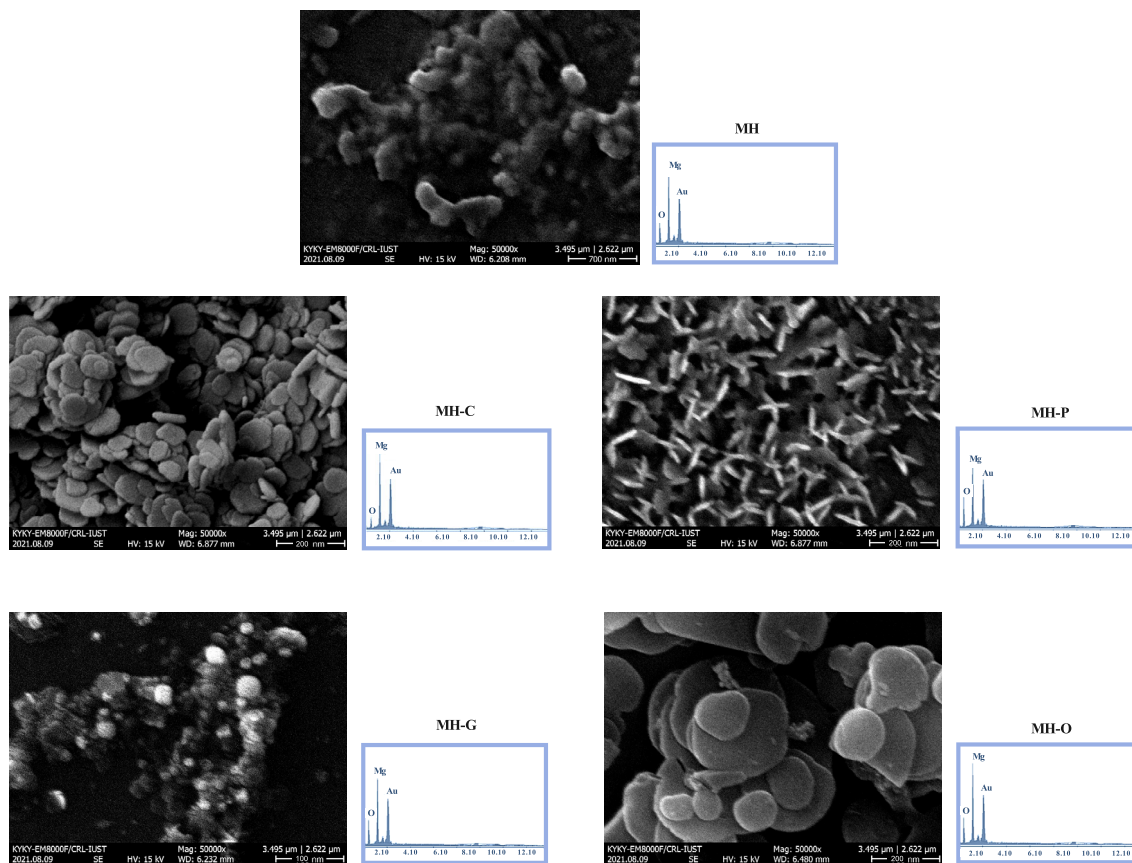


**Fig. 4:** FESEM and EDS analyses of MH powders. While the MH powder without any surfactant was completely agglomerated, the rest of the powders were completely dispersed and were observed with nano-flake (MH-C), nano-plate (MH-P), nano-spherical (MH-G), and nano-disk (MH-O) morphologies. Mg, O, and Au peaks were identified in all EDS graphs

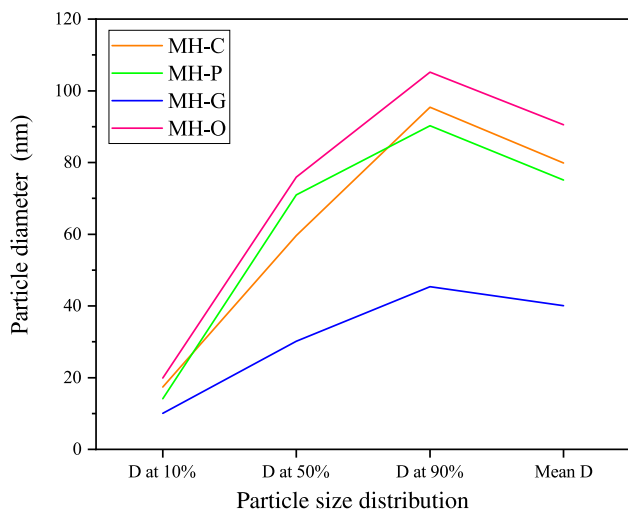


**Fig. 5:** Effect of applying different surfactants on diameter in different volumes of particles. Curves were extracted from dynamic light scattering analysis

ities is what is meant by thermal stability.<sup>54</sup> Thermal degradation of PU which is attributed to absorbed thermal energy, constitutes an important phenomenon from both a fundamental and a technological perspective.<sup>55</sup> The thermal, oxidation, and fire resistancy of different types of PU play a significant role in their functional determining.<sup>56</sup>

According to fundamental studies, the thermal degradation of PU is a complicated heterogeneous phenomenon that involves a multitude of partial decomposition reactions. The side products formation and the onset decomposition temperature are both significantly influenced by changing the isocyanate to hydroxyl (NCO:OH) ratio. It has also been demonstrated that the weight loss during decomposition increases with the oxygen content of polyol. According to the constant NCO:OH ratio in this study (1:2), the decomposition temperature is expected to be between 250–300 °C.<sup>57,58</sup>

A wide range of fillers have been studied to enhance PU polymers. Generally, PU thermal stability improvement tends to depend on the size, shape, type,

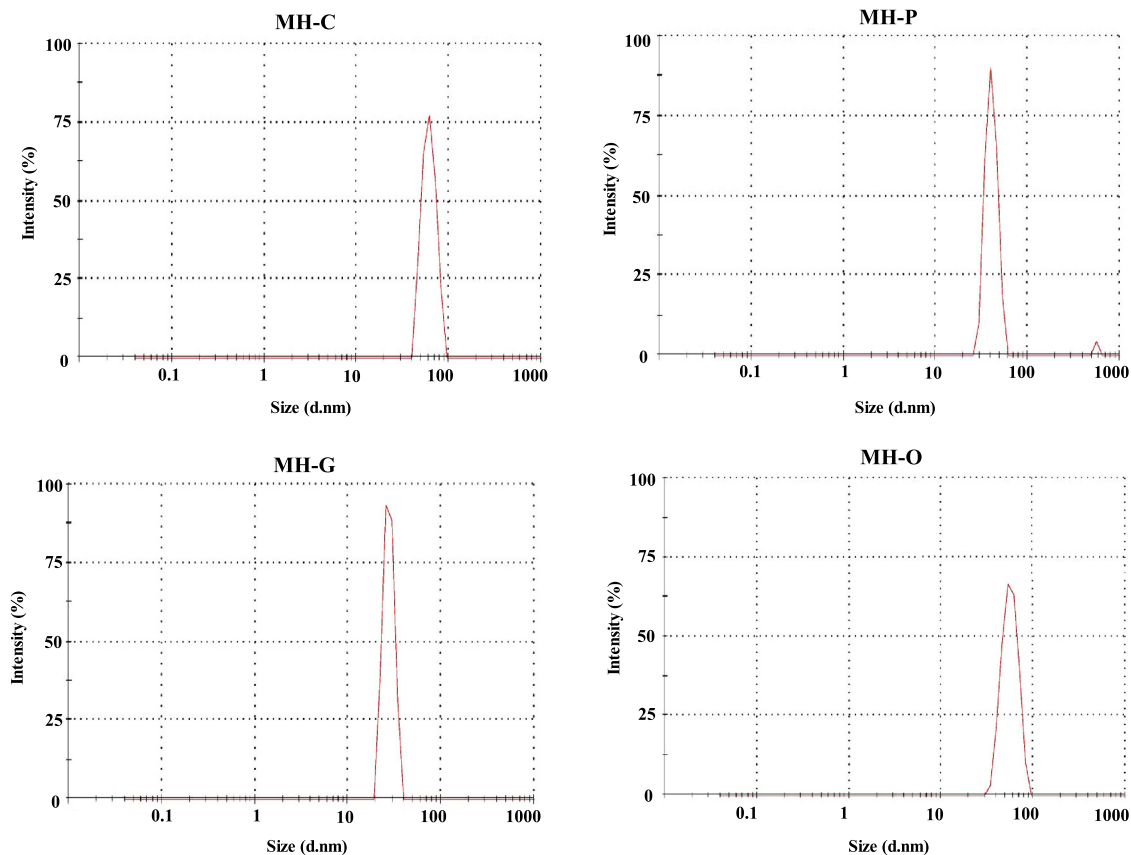


**Fig. 6: DLS analysis of MH powders synthesized with four different surfactants. Particle size distribution was observed between 60 and 100 nm in MH-C, 80 and 90 nm in MH-P, 30 and 45 nm in MH-G, and 75 and 105 nm in MH-O**

amount, dispersion of applied filler, as well as filler-matrix interaction. The high surface area of nanofillers results in increasing the interfacial interaction and reducing the heat release rate of the polymers. Therefore, high thermal stability could be obtained by applying modified inorganic nanofillers that are uniformly dispersed throughout the organic matrix and interact strongly with it.<sup>54-58</sup>

According to Fig. 9, the decomposition temperature for PU is about 275 °C and increased to 300 °C via addition of nano-MH. Due to the extra fine dimensions of MH-G and the greater contact surface with the polymer matrix, the decomposition temperature in PU-G is the highest (approximately 300 °C), while it varies around 280-285 °C for the rest of the nanocomposites. Indeed, particle sizes of MH-C, MH-P, and MH-O were not that much different to create a significant change in DTA analysis. Although, the fire resistance of MH improved the thermal stability of PU due to the presence of -OH bond in the chemical structure of Mg(OH)<sub>2</sub>.

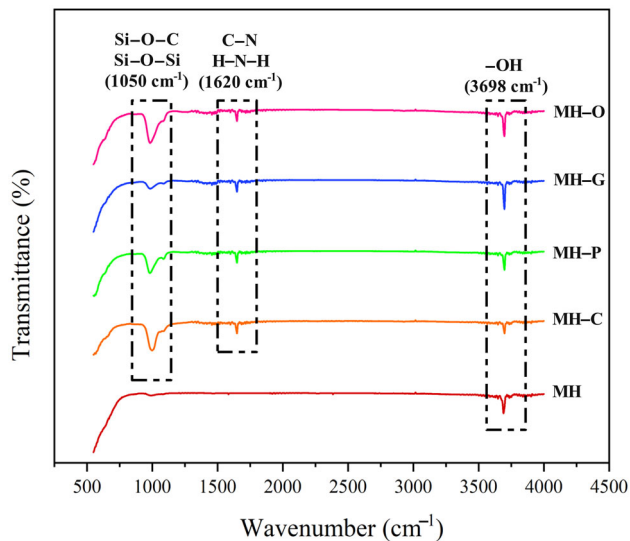


**Fig. 7: FTIR spectra of modified nano-MH powders with APTES**

**Table 4: Synthesized MH powder properties**

Sample code	Surfactant	Morphology	Particle size (nm)
MH	–	Agglomerate	–
MH-C	CTAB	Flake	79.86
MH-P	PEG500	Plate	75.09
MH-G	Gelatin	Spherical	40.07
MH-O	Oleic Acid	Disk	90.5

### Hydrophobicity analysis

**Static contact angle.** By evaluating the static contact angle (Fig. 10), the impact of adding MH with different morphologies on the hydrophobicity of PU was examined. Referring to Fig. 11, the average contact angle of  $63.5^\circ \pm 0.5$  in PU increased to  $132.4^\circ \pm 0.4$ ,  $142.3^\circ \pm 0.2$ ,  $130.7^\circ \pm 0.2$ , and  $135.5^\circ \pm 0.4$  by applying MH-C, MH-P, MH-G, and MH-O, respectively. All nanocomposite samples have a higher contact angle than pure PU. In general, the surface is hydrophobic if a drop of water tends to stick to itself more than the substrate. Herein, the contact angle is above  $90^\circ$ . On the other hand, if a drop of water tends to stick to the substrate instead of itself, the surface will be hydrophilic, and the contact angle is below  $90^\circ$ .<sup>59</sup> In terms of wettability characteristics, PU is neither totally hydrophilic nor totally hydrophobic. If its behavior can switch from being more hydrophilic or more hydrophobic, its application field will be expanded. It is thus exceedingly complicated to turn it into a superhydrophobic substance.<sup>41</sup>

A wide range of research has noted that adding nanofillers to PU could increase surface roughness and consequently enhance contact angle. Various researchers have demonstrated that if nanoparticles and low surface energy elements are added to a polymer matrix, hydrophobicity can be increased.<sup>23,29</sup> However, based on references, employing fillers in optimum content will be efficient, whereas more that it will have the opposite effect.<sup>60</sup> According to the lotus theory, there are many inequalities on the surface. When a drop of water falls on the surface, a certain amount of air will be trapped between inequalities and increases the contact angle.<sup>61</sup> Indeed, increasing roughness on thin film surfaces with a hydrophilic nature such as PU, and then modifying it with low-energy materials such as functionalized nanofillers leads to an increment in the specific surface area and ultimately improves the contact angle and hydrophobicity.

Based on past studies, researchers have focused more on two parameters, the amount and size of nanoparticles on the polymer surface. While at a

constant percentage, the shape of nanoparticles can also affect the surface roughness. In other words, the existence of nanoparticles with different morphologies on the surface can create different inequalities, which will cause a difference in surface roughness. To increase hydrophobicity, either the molecular structure of the polyurethane must be modified during synthesis, or hydrophobic additives must be applied to the composition of the PU. Superhydrophobic PU surfaces cannot be produced on a widespread basis using the first method since it is more challenging and costly.<sup>62</sup> In previous studies, by adding different nanofillers to the PU matrix, a contact angle of  $105^\circ$  has been obtained. This improvement in water repellency from the initial value of  $65^\circ$  has been obtained only by changing the percentage of reinforcement in the composite.<sup>41</sup> While in this study, only by changing the shape of the nanofiller, the contact angle improved by 130% and reached from  $62^\circ$  to  $142^\circ$ . As anticipated from the FESEM (Fig. 8), the added nano-MH with different morphologies caused different inequalities and made significant changes on the surface roughness, and as a result, contact angle. According to the mechanism proposed in Fig. 12, the existence of nano-flake, nano-plate, nano-spherical, and nano-disk of MH created different ups and downs on thin film surface. These irregularities affect the shape of the water droplet in contact with the surface. The shape of a liquid-vapor interface is determined by the Young equation:

$$\gamma_{SG} - \gamma_{SL} - \gamma_{LG} \cos \theta_{C=0} \quad (5)$$

Where  $\gamma_{SG}$ ,  $\gamma_{SL}$ ,  $\gamma_{LG}$ , and  $\theta_C$  indicate solid-gas interfacial energy, solid-liquid interfacial energy, liquid-gas interfacial energy, and equilibrium contact angle, respectively. The consideration of thermodynamic equilibrium between the three phases-liquid (L), solid (S), and gas or vapor (G)-gives birth to the theoretical description of the contact. Surface wettability and contact angle are significantly impacted by surface roughness. The impact of roughness depends on whether the droplet fills in surface ridges or leaves air spaces between it and the surface.<sup>63</sup> Since in thin films, nanoparticles are more on the surface than in the depth, their morphology can change the trapped air spaces between the water droplet and the surface. For example, in the PU-C sample, which contains 80 nm flakes with random distribution, the air spaces are created so that the droplet tends to bulge out in order to reduce its contact area with the surface. Conversely, water droplets spread out on the surface and displayed low contact angles when the surface was hydrophilic in the pure PU sample.

To improve the PU hydrophobicity, adding large amounts of fillers should be avoided. The variant

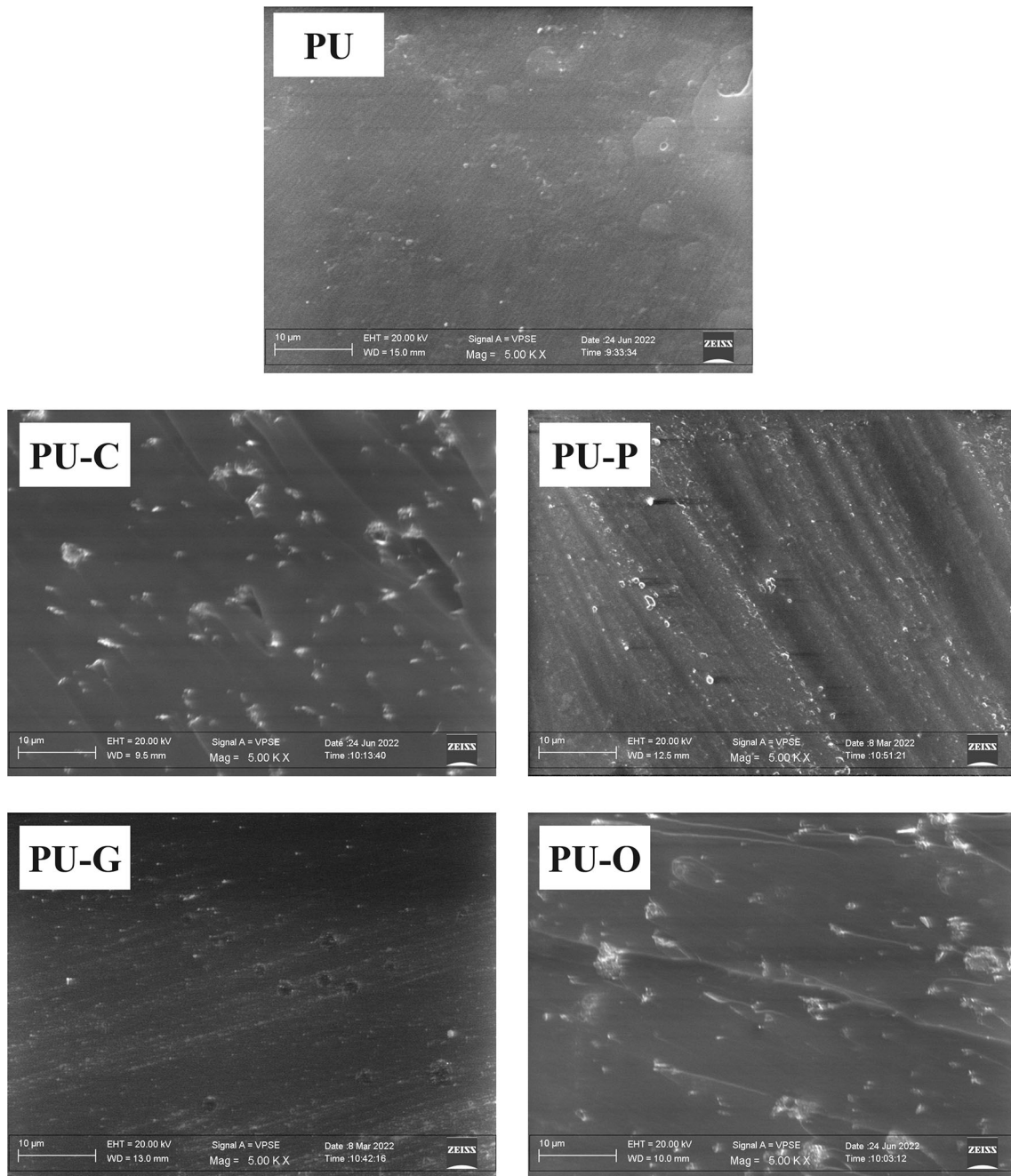


**Fig. 8: FESEM images of PU/Mg(OH)<sub>2</sub> nanocomposite samples**

densities cause nanofillers to pass through the coating's exterior and create different topographies. On the other hand, one of the most important ways to improve hydrophobicity is to add a hydrophobic agent to nanoparticles and modify the surface, for example, with APTES. By modifying the surface, agglomeration of nanofillers will be prevented. In this case, the effect of their morphology on surface roughness and water

contact angle will be more visible.<sup>49,64</sup> In other words, when the surface energy of the solid equals those of the liquid, water droplets have a tendency to wet the solid to establish the balance of equation (5). The same has happened in all nanocomposites except in PU-G, which contains very fine nanoparticles. In this sample, less air space is created between the water droplet and the surface, and the contact angle is less improved than in

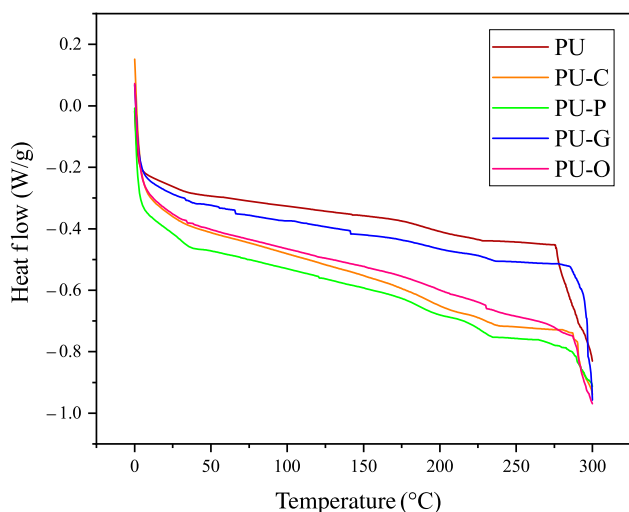


Fig. 9: Differential scanning calorimetric analysis of PU/Mg(OH)<sub>2</sub> nanocomposite samples

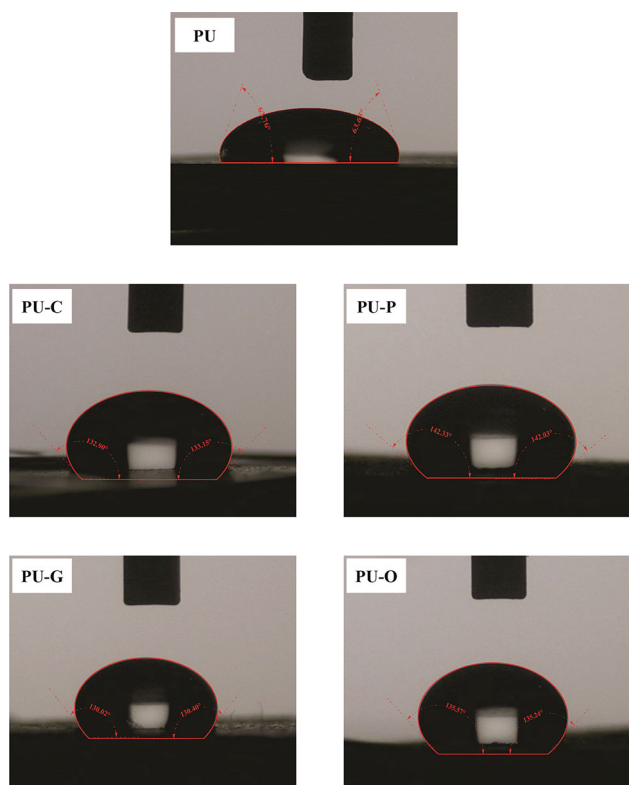


Fig. 10: Static contact angle of PU/Mg(OH)<sub>2</sub> nanocomposite samples

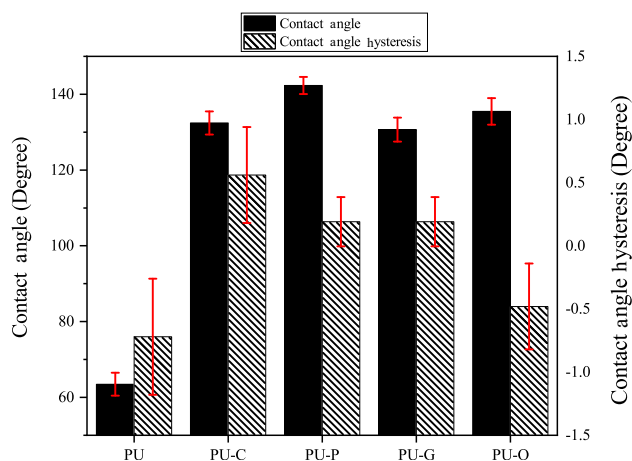


Fig. 11: Alterations in the hydrophobicity of PU/Mg(OH)<sub>2</sub> nanocomposite samples

others. However, in PU-P, with the special orientation of nano-plates on the surface, a regular and more air space is formed and the water droplet has strongly aggregated.

Surface roughness

AFM. Figure 13 illustrates the AFM images of the pure PU and nanocomposites containing 3% w.t. MH with different morphologies. The results obtained from FESEM images (Fig. 8) and contact angle (Fig. 10) are confirmed with AFM images.

By comparing the surface of samples containing nano-flake and nano-plate (PU-C and PU-P) with the surface of samples containing nano-spherical and nano-disk (PU-G and PU-O), it is determined that the particles with sharp corners have created a rougher surface. This variability in surface roughness could affected contact angle. The significant increase in the static contact angle of PU-P is due to the vertical orientation of MH-P on the surface. This surface structure could trap air, create more air space between water droplet and surface, to bulge out the droplet, increase contact angle, and finally enhance the hydrophobicity. Without any roughness in nano or microscale, it is nearly impossible to achieve a contact angle of more than 120° on a smooth surface (just by surface chemical modification). Surface roughness is thus a crucial component of hydrophobic coatings. There are two regimes that describe contact angle enhancement due to surface roughness and topography: Wenzel and Cassie-Baxter. Whereas the contact

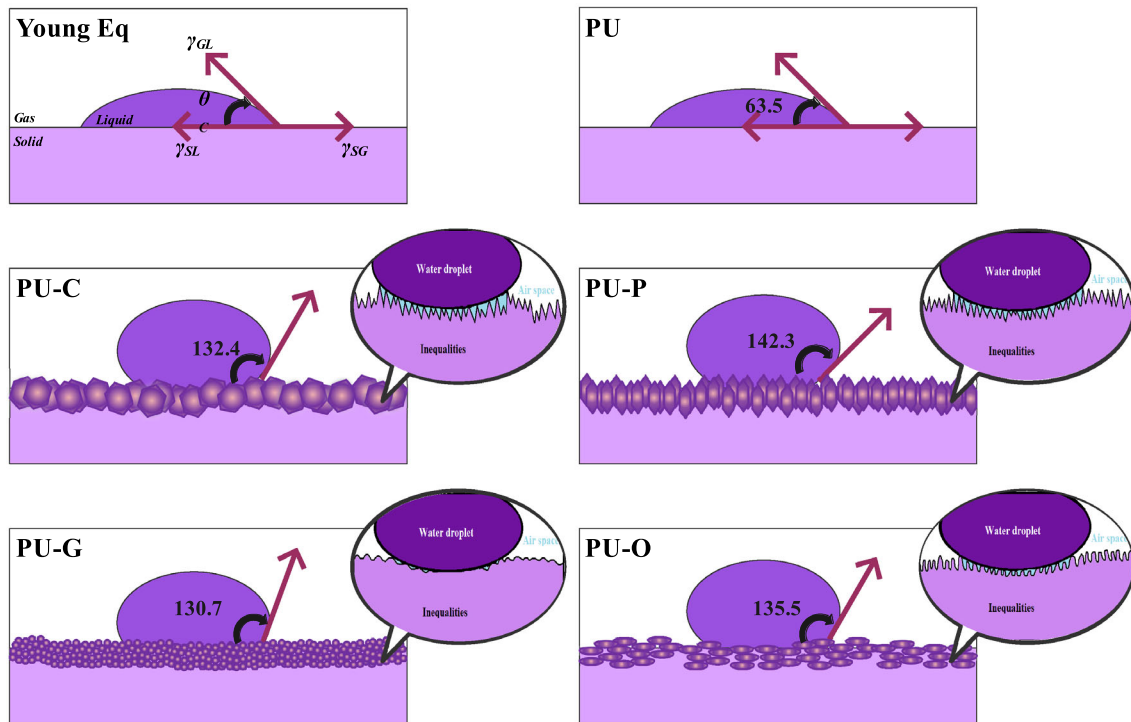


Fig. 12: Schematic presenting the impact of nano-MH morphology on surface wettability and water droplet contact angle

angle improves with surface roughness in both regimes, the Cassie-Baxter is more affected by trapped air spaces in the surface inequalities, which could impact the contact angle and improve hydrophobicity.<sup>65,66</sup>

### Mechanical properties

**Hardness.** Figure 14 compares the hardness variation of pure PU with the rest of the nanocomposites. This test indicates that hardness has improved from 60 Shore A for pure PU sample to a maximum level of 88 Shore A for the PU-P sample. This increment refers to the presence of MH hard particles inside the soft PU matrix.<sup>16</sup> Hardness is considered as a low strain modulus and it will enhance by increasing filler steadily.<sup>13</sup> According to the constant content of nanoparticles in all samples and the dependence of hardness on the amount of reinforcement in the matrix, no noticeable change in the hardness of nanocomposites can be observed by different morphologies.

**Tensile properties.** Stress-strain curves of pure PU and nanocomposite are compared in Fig. 15. The mechanical properties of PU-P are more improved than other samples due to the greater interaction of MH-P with PU chains. Although the uniform distribution and preferential orientation of nanoparticles in the

polymer matrix have also been effective in mechanical strength.

As can be seen from tensile test results in Fig. 16, nanocomposites exhibit better mechanical properties than pure PU. The load transfer rate at the filler-polymer interface and, consequently, the composite's final strength are enhanced by uniformly dispersed and distributed reinforcements in the polymer matrix. Additionally, it has been demonstrated that tiny but multiple pinning spots can prevent cracks from growing and expanding. As physical crosslinkers, nanoparticles limit the mobility of PU chains while improving tensile modulus and strength. The tensile modulus and strength will decrease as the strain increases because weak spots and cracks will develop at high nanoparticle concentrations and the strain force will be distributed irregularly. By adding reinforcement particles or raising their content in the polymer matrix, elongation at break is typically lowered. The type, amount, and bond strength of the reinforcement with the polymer determine mechanical properties including strength and fracture strain.<sup>16,41</sup> Although in this research, only the morphology of nano-MH was changed and the content and type of reinforcement were constant, differences between the nanocomposites are still observed. It seems that the best mechanical properties belong to the PU-P which contains nano-plate with vertical orientation.

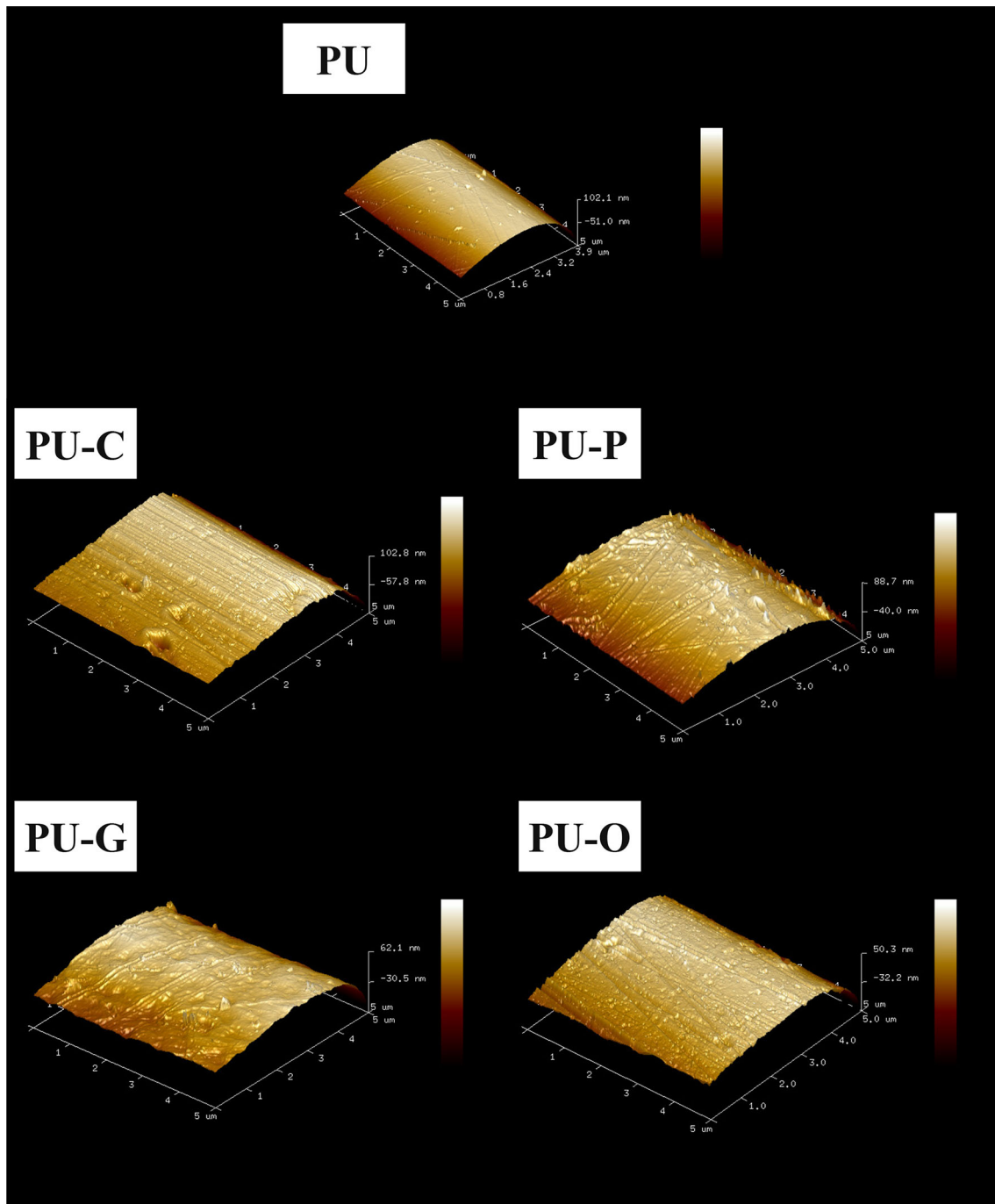
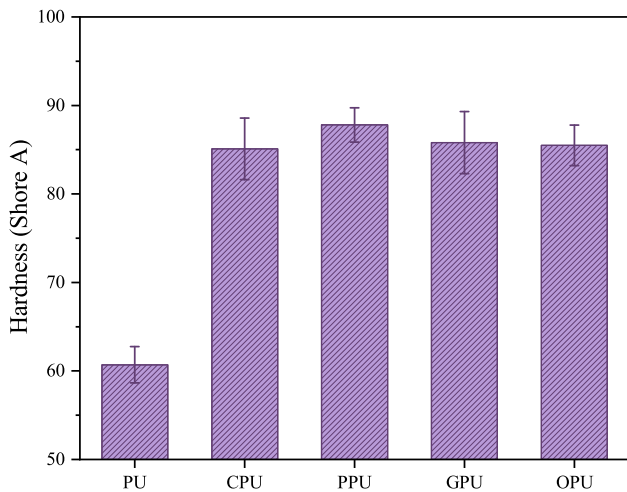


Fig. 13: The trend of surface roughness changes in PU composite samples by adding different morphologies of  $\text{Mg}(\text{OH})_2$

*Fracture surface characterization.* Figure 17 shows FESEM fracture surface on stress-strain samples to explain the deformation and fracture behavior. It is inferred from these images that the presence of nano-

MH has increased the surface roughness and brittleness of the fracture.

Based on the previous discussions, nano-MH causes more intermolecular interactions between PU chains. As this leads to a decrease in flexibility and a stiffness



**Fig. 14: Comparison of hardness values on the Shore A scale of PU/Mg(OH)<sub>2</sub> nanocomposite samples**

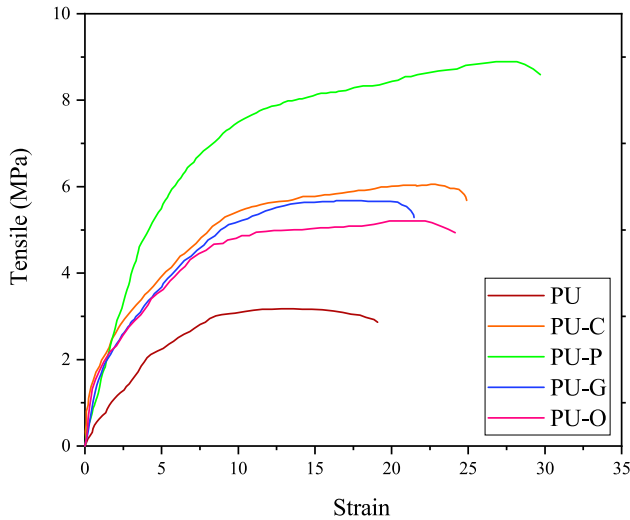


**Fig. 15: Stress-strain curves of PU/Mg(OH)<sub>2</sub> nanocomposite samples**

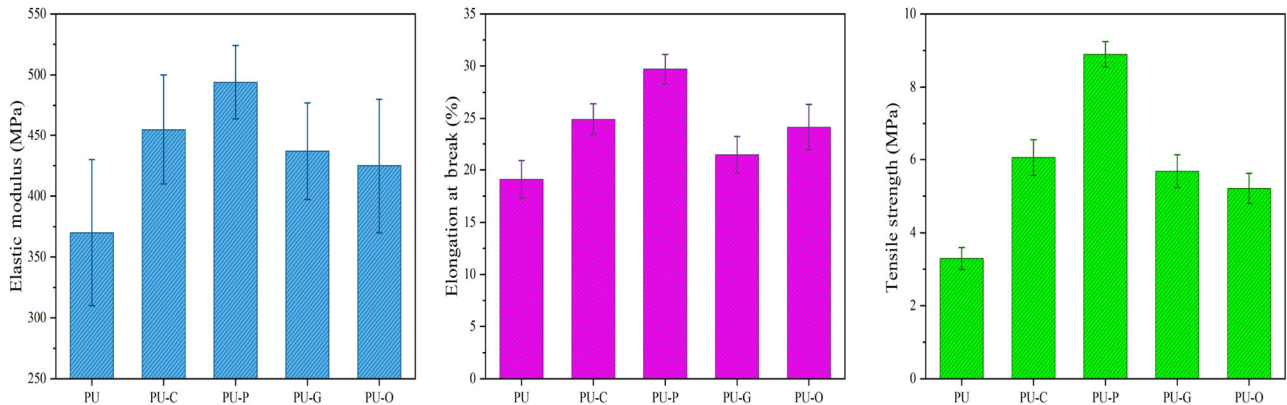


**Fig. 16: Elastic modulus, elongation at break, and tensile strength variations of PU/Mg(OH)<sub>2</sub> nanocomposite samples**

increment in the filler-polymer interface, large and rough ruggedness is observed at the fracture surface of nanocomposites. Of course, this happened less in two samples containing nano-MH with rounded corners (PU-G and PU-O).

### Conclusions

The primary purpose of this study was to evaluate the impact of nano-MH morphologies on the hydrophobicity, physical, and mechanical properties of PU composites. In this regard, different morphologies of nano-MH were obtained by a hydrothermal method at 180 °C for 18 h with the addition of four surfactants: CTAB, PEG500, gelatin, and oleic acid. Synthesized nano-MH was examined by XRD, FESEM, DLS, and FTIR. Nano-flake, nano-plate, nano-spherical, and nano-disk morphologies of MH were applied in PU matrix by drop casting method. Then, microstructure, thermal stability, surface characterization, hydrophobicity, and mechanical properties of nanocomposites were compared with pure PU. The observations indicated that different surface topographies would result from the presence of nanoparticles with various morphologies on the nanocomposite’s surface. The shape, size, and orientation of MH on the nanocomposite surface establish various topographies, which have a direct impact on hydrophobicity. Extremely high water contact angles were attained as a result of the surface roughness, revealing the superhydrophobic behavior of the produced nanocoatings. Also, the presence of MH in PU matrix improved the mechanical properties of the nanocomposite, depending on the aspect ratio and particle size. Therefore, hardness, tensile strength, elastic modulus, and elongation at break in the best nanocomposite (PU-P) improved by 47%, 170%, 34%, and 56%, respectively. Finally, this paper demonstrated that the vertical orientation of MH-P allowed for obtaining the highest hydrophobicity in the PU-P sample.



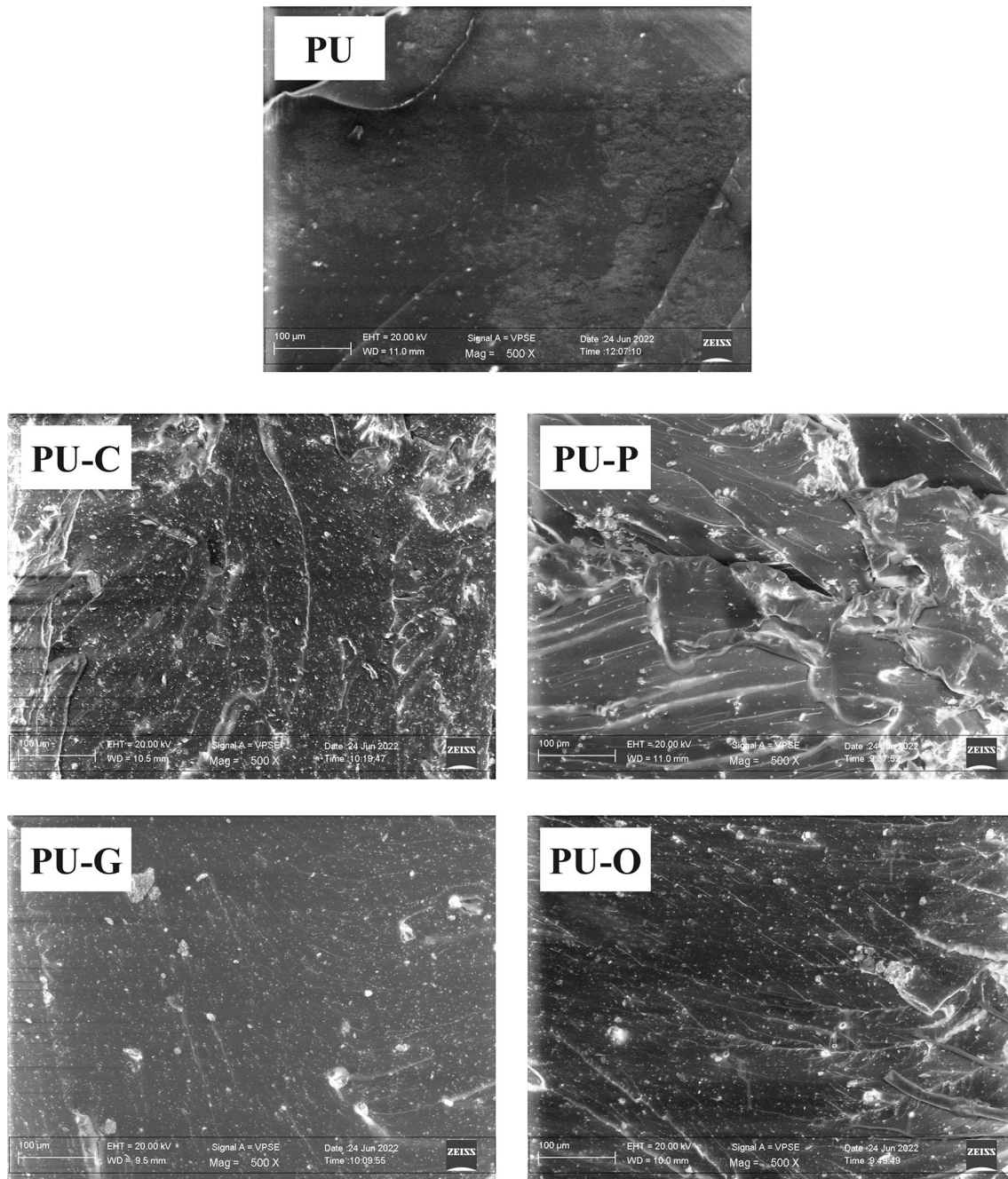


Fig. 17: FESEM-fractured surface of PU/Mg(OH)<sub>2</sub> nanocomposite samples

**Conflict of interest** The authors declare that they have no known competing financial interests or personal relationships that could have appeared to influence the work reported in this paper.

## References

1. Zhang, Z, Du, J, Li, J, Huang, X, Kang, T, Zhang, C, Wang, S, Ajao, OO, Wang, W-J, Liu, P, “Polymer Nanocomposites with Aligned Two-Dimensional Materials.” *Prog. Polym. Sci.*, **114** 101360 (2021)
2. Pavlidou, S, Papaspyrides, C, “A Review on Polymer-Layered Silicate Nanocomposites.” *Prog. Polym. Sci.*, **33** (12) 119–1198 (2008)
3. Kausar, A, “Strategies in Polymeric Nanoparticles and Hybrid Polymer Nanoparticles.” *NanoWorld J.*, **5** (1) 1–5 (2019)
4. Soucek, M, Zong, Z, Johnson, A, “Inorganic/Organic Nanocomposite Coatings: The Next Step in Coating Performance.” *JCT Res.*, **3** (2) 133–140 (2006)

5. Kausar, A, “Polyurethane Composite Foams in High-Performance Applications: A Review.” *Polym.-Plastics Technol. Eng.*, **57** (4) 346–369 (2018)
6. Ji, M, Huang, J, Zhu, C, “Methods for Synthesizing Polymer Nanocomposites and Their Applications.” *Funct. Nanomater. Synthesis, Properties, Appl.*, 447–490 (2022)
7. Chattopadhyay, DK, Raju, K, “Structural Engineering of Polyurethane Coatings for High Performance Applications.” *Prog. Polym. Sci.*, **32** (3) 352–418 (2007)
8. Jing, Q, Liu, W, Pan, Y, Silberschmidt, VV, Li, L, Dong, Z, “Chemical Functionalization of Graphene Oxide for Improving Mechanical and Thermal Properties of Polyurethane Composites.” *Mater. Design*, **85** 808–814 (2015)
9. Suleman, S, Khan, SM, Gull, N, Aleem, W, Shafiq, M, Jamil, T, “A Comprehensive Short Review on Polyurethane Foam.” *Int. J. Innov. Sci. Res.*, **12** 165–169 (2014)
10. Kausar, A, “Polyurethane Nanocomposite Coatings: State of the Art and Perspectives.” *Polym. Int.*, **67** (11) 1470–1477 (2018)
11. Xiong, J, Zheng, Z, Qin, X, Li, M, Li, H, Wang, X, “The Thermal and Mechanical Properties of a Polyurethane/Multi-Walled Carbon Nanotube Composite.” *Carbon*, **44** (13) 2701–2707 (2006)
12. Zia, F, Zia, KM, Aftab, W, Tabasum, S, Asrar, M, et al., “Synthesis and Characterization of Hydroxyethyl Cellulose Copolymer Modified Polyurethane Bionanocomposites.” *Int. J. Biol. Macromol.*, **179** 345–352 (2021)
13. Allami, T, Alamiery, A, Nassir, MH, Kadhum, AH, “Investigating Physio-Thermo-Mechanical Properties of Polyurethane and Thermoplastics Nanocomposite in Various Applications.” *Polymers*, **13** (15) 2467 (2021)
14. Ciecierska, E, Jurczyk-Kowalska, M, Bazarnik, P, Gloc, M, Kulesza, M, Kowalski, M, Krauze, S, Lewandowska, M, “Flammability, Mechanical Properties and Structure of Rigid Polyurethane Foams with Different Types of Carbon Reinforcing Materials.” *Compos. Struct.*, **140** 67–76 (2016)
15. Subhani, T, Latif, M, Ahmad, I, Rakha, SA, Ali, N, Khurram, AA, “Mechanical Performance of Epoxy Matrix Hybrid Nanocomposites Containing Carbon Nanotubes and Nanodiamonds.” *Mater. Design*, **87** 436–444 (2015)
16. Albozahid, M, Naji, HZ, Alobad, ZK, Saiani, A, “Enhanced Mechanical, Crystallisation and Thermal Properties of Graphene Flake-Filled Polyurethane Nanocomposites: The Impact of Thermal Treatment on the Resulting Microphase-Separated Structure.” *J. Polym. Res.*, **28** (8) 1–16 (2021)
17. Ma, Z, Li, Q, Wei, J, Liang, C, Yang, T, Wang, G, Xia, C, “Effects of Al-Based Alloy Powders on the Mechanical Behavior, Corrosion Resistance and Infrared Emissivity of Polyurethane Composite Coatings.” *Coll. Surfaces A: Physicochem. Eng. Aspects*, **624** 126782 (2021)
18. Maganty, S, Roma, MP, Meschter, SJ, Starkey, D, Gomez, M, Edwards, DG, Ekin, A, Elskan, K, Cho, J, “Enhanced Mechanical Properties of Polyurethane Composite Coatings Through Nanosilica Addition.” *Prog. Org. Coat.*, **90** 243–251 (2016)
19. Chattopadhyay, D, Webster, DC, “Thermal Stability and Flame Retardancy of Polyurethanes.” *Prog. Polym. Sci.*, **34** (10) 1068–1133 (2009)
20. Mogha, A, “Clay and Carbon Nanotubes as the Potential Fillers for Polyurethanes for Flame-Retardant Coatings.” In: *Materials and Chemistry of Flame-Retardant Polyurethanes Volume 2: Green Flame Retardants 2* pp. 31–45. ACS Publications, (2021)
21. Peng, S, Iroh, JO, “Dependence of the Dynamic Mechanical Properties and Structure of Polyurethane-Clay Nanocomposites on the Weight Fraction of Clay.” *J. Compos. Sci.*, **6** (6) 173 (2022)
22. Skosana, SJ, Khoathane, C, Malwela, T, “Enhancing the Adhesion Strength of Polyurethane Coatings by Dispersing Layered Silicates via Sonication and High-Shear Mixing Method.” *Polym. Bull.*, **78** (1) 203–221 (2021)
23. Sitthisuwannakul, K, Boonpavanitchakul, K, Wirunmongkol, T, Muthitamongkol, P, Kangwansupamonkon, W, “A Tunable Controlled-Release Urea Fertilizer Coated with a Biodegradable Polyurethane-Nanoclay Composite Layer.” *J. Coat. Technol. Res.*, 1–12 (2022)
24. Huang, W, Huang, J, Yu, B, Meng, Y, Cao, X, Zhang, Q, Wu, W, Shi, D, Jiang, T, Li, RK, “Facile Preparation of Phosphorus Containing Hyperbranched Polysiloxane Grafted Graphene Oxide Hybrid Toward Simultaneously Enhanced Flame Retardancy and Smoke Suppression of Thermoplastic Polyurethane Nanocomposites.” *Compos. Part A: Appl. Sci. Manuf.*, **150** 106614 (2021)
25. Awasthi, S, Agarwal, D, “Influence of Cycloaliphatic Compounds on the Properties of Polyurethane Coatings.” *J. Coat. Technol. Res.*, **4** (1) 67–73 (2007)
26. Naiker, VE., Mestry, S, Nirgude, T, Gadgeel, A, Mhaske, S, “Recent Developments in Phosphorous-Containing Bio-Based Flame-Retardant (FR) Materials for Coatings: An Attentive Review.” *J. Coat. Technol. Res.*, **20**, 113–139 (2023)
27. Awad, MA, Saleh, N, Elsayy, M, Salem, SS, El-Wahab, A et al, “Preparation of Polyurethane Coating Formulation Based on Dihydropyridine Derivatives as an Insecticide and Antifungal Additives for Surface Coating Applications.” *J. Coat. Technol. Res.*, 1–13 (2022)
28. Zhang, J, Zhang, N, Liu, Q, Ren, H, Li, P, Yang, K, “Investigation of Hybrid Materials Based on Polyurethane Modified with Aliphatic Side Chains Combined with Nano-TiO<sub>2</sub>.” *Aus. J. Chem.*, **71** (1) 47–57 (2017)
29. Awais, M, Jalil, M, Zulfqar, U, Husain, S, “A Facile Approach Towards Fabrication of Super Hydrophobic Surface from Functionalized Silica Particles.” In: IOP Conference Series: Materials Science and Engineering, **146** 012022 (2016)
30. Soleimani, E, Taheri, R, “Synthesis and Surface Modification of CuO Nanoparticles: Evaluation of Dispersion and Lipophilic Properties.” *Nano-Struct. Nano-Objects*, **10** 167–175 (2017)
31. Wang, Z, Liu, F, Han, E, Ke, W, Luo, S, “Effect of ZnO Nanoparticles on Anti-Aging Properties of Polyurethane Coating.” *Chin. Sci. Bull.*, **54** (19) 3464–3472 (2009)
32. El Saeed, AM, Abd El-Fattah, M, Azzam, AM, “Synthesis of ZnO Nanoparticles and Studying Its Influence on the Antimicrobial, Anticorrosion and Mechanical Behavior of Polyurethane Composite for Surface Coating.” *Dyes and Pigments*, **121** 282–289 (2015)
33. Bui, TMA, Nguyen, TV, Nguyen, TM, Hoang, TH, Nguyen, TTH, Lai, TH, Tran, TN, Hoang, VH, Le, TL, Dang, TC, et al. “Investigation of Crosslinking, Mechanical Properties and Weathering Stability of Acrylic Polyurethane Coating Reinforced by SiO<sub>2</sub> Nanoparticles Issued from Rice Husk Ash.” *Mater. Chem. Phys.*, **241** 122445 (2020)
34. Song, H-J, Zhang, Z-Z, Men, X-H, “The Tribological Behaviors of the Polyurethane Coating Filled with Nano-SiO<sub>2</sub> Under Different Lubrication Conditions.” *Compos. Part A: Appl. Sci. Manuf.*, **39** (2) 188–194 (2008)
35. Nguyen, TV, Nguyen, TA, Dao, PH, Nguyen, AH., Do, MT, et al. “Effect of Rutile Titania Dioxide Nanoparticles on the Mechanical Property, Thermal Stability, Weathering Resistance and Antibacterial Property of Styrene Acrylic Poly-

- urethane Coating.” *Adv. Natural Sci. Nanosci. Nanotechnol.*, **7** (4) 045015 (2016)
36. Sabzi, M, Mirabedini, S, Zohuriaan-Mehr, J, Atai, M, “Surface Modification of TiO<sub>2</sub> Nano-Particles with Silane Coupling Agent and Investigation of its Effect on the Properties of Polyurethane Composite Coating.” *Prog. Org. Coat.*, **65** (2) 222–228 (2009)
  37. Liu, S, Wei, X, Lin, S, Guo, M, “Preparation of Aerogel Mg(OH)<sub>2</sub> Nanosheets by a Combined Sol-Gel-Hydrothermal Process and its Calcined mgo Towards Enhanced Degradation of Paraoxon Pollutants.” *J. Sol-Gel Sci. Technol.*, **99** (1) 122–131 (2021)
  38. Chen, Y, Zhou, T, Fang, H, Li, S, Yao, Y, He, Y, “A Novel Preparation of Nano-Sized Hexagonal Mg(OH)<sub>2</sub>.” *Proc. Eng.*, **102** 388–394 (2015)
  39. Ding, Y, Zhang, G, Wu, H, Hai, B, Wang, L, Qian, Y, “Nanoscale Magnesium Hydroxide and Magnesium Oxide Powders: Control Over Size, Shape, and Structure via Hydrothermal Synthesis.” *Chem. Mater.*, **13** (2) 435–440 (2001)
  40. Feng, S-H, Li, G-H, “Hydrothermal and Solvothermal Syntheses.” In: *Modern Inorganic Synthetic Chemistry*, pp. 73–104. Elsevier, (2017)
  41. Sohrabi-Kashani, L, Yekta, BE, Rezaie, HR, Zolriasatein, A, “Synergistic Effect of Micro-and Nano-TiO<sub>2</sub> on Hydrophobic, Mechanical, and Electrical Properties of Hybrid Polyurethane Composites.” *J. Materi. Sci. Mater. Electron.*, 1–20 (2022)
  42. Seyedmehdi, S, Ebrahimi, M, “Superhydrophobic Modified-Polyurethane Coatings for Bushing of Power Transformers: From Material to Fabrication, Mechanical and Electrical Properties.” *Prog. Org. Coat.*, **123** 134–137 (2018)
  43. Yousefi, S, Ghasemi, B, “Ultrasound-assisted Synthesis of Porous Mg(OH)<sub>2</sub> Nanostructures Using Hypersaline Brine.” *Micro & Nano Lett.*, **14** (9) 1019–1023 (2019)
  44. Wu, H, Luo, B, Gao, C, Wang, L, Wang, Y, Zhang, Q, “Synthesis and Size Control of Monodisperse Magnesium Hydroxide Nanoparticles by Microemulsion Method.” *J. Dispersion Sci. Technol.*, (2019)
  45. Erciyes, A, Andac, M, “Synthesis and Characterization of Nano-Sized Magnesium 1, 4-Benzenedicarboxylate Metal Organic Framework via Electrochemical Method.” *J. Solid State Chem.*, **309** 122970 (2022)
  46. Sharma, D, Ledwani, L, Kumar, N, Pervaiz, N, Mehrotra, T, Kumar, R, “Structural and Physicochemical Properties of Rheum Emodi Mediated Mg(OH)<sub>2</sub> Nanoparticles and Their Antibacterial and Cytotoxic Potential.” *IET Nanobiotechnol.*, **14** (9) 858–863 (2020)
  47. Yousefi, S, Ghasemi, B, “Mg(OH)<sub>2</sub> Nanostructures Using Impure Brine: Optimization of Synthesis Parameters by Taguchi Robust Design and Study of Optical Properties.” *Res. Chem. Intermediat.*, **47** (5) 2029–2047 (2021)
  48. Babar, M, Sharma, A, Kakkar, P, Arora, A, Arora, T, Verma, G, “Correlating Thermal Properties of Polyurethane/clay Nanocomposite Coatings with Processing.” *Prog. Org. Coat.*, **165** 106743 (2022)
  49. Sharma, A, Babar, M, Kakkar, P, Gahlout, P, Verma, G, “Correlating Mechanical Properties of Polyurethane-Organoclay Nanocomposite Coatings with Processing.” *Prog. Org. Coat.*, **169** 106895 (2022)
  50. Nayak, N, Huertas, R, Crespo, JG, Portugal, CA, “Surface Modification of Alumina Monolithic Columns with 3-Aminopropyltetraethoxysilane (APTES) for Protein Attachment.” *Sep. Purif. Technol.*, **229** 115674 (2019)
  51. Zahir, MH, Rahman, MM, Irshad, K, Rahman, MM, “Shape-Stabilized Phase Change Materials for Solar Energy Storage: MgO and Mg(OH)<sub>2</sub> Mixed with Polyethylene Glycol.” *Nanomaterials*, **9** (12) 1773 (2019)
  52. Zhang, M, Song, W, Chen, Q, Miao, B, He, W, “One-Pot Synthesis of Magnetic Ni@Mg(OH)<sub>2</sub> Core-Shell Nanocomposites as a Recyclable Removal Agent for Heavy Metals.” *ACS Appl. Mater. Interfaces*, **7** (3) 1533–1540 (2015)
  53. Vafaefard, M, Ibrahim, S, Wong, KT, Pasbakhsh, P, Pichiah, S, Choi, J, Yoon, Y, Jang, M, “Novel Self-Assembled 3d Flower-Like Magnesium Hydroxide Coated Granular Polyurethane: Implication of its Potential Application for the Removal of Heavy Metals.” *J. Clean. Prod.*, **216** 495–503 (2019)
  54. Akindoyo, JO, Beg, M, Ghazali, S, Islam, M, Jeyaratnam, N, Yuvaraj, A, “Polyurethane Types, Synthesis and Applications-A Review.” *RSC Adv.*, **6** (115) 114453–114482 (2016)
  55. Pielichowski, K, Słotwińska, D, Dziwiński, E, “Segmented MDI/HMDI-Based Polyurethanes with Lowered Flammability.” *J. Appl. Polym. Sci.*, **91** (5) 3214–3224 (2004)
  56. Barendregt, R, Van Den Berg, P, “The Degradation of Polyurethane.” *Thermochimica Acta*, **38** (2) 181–195 (1980)
  57. Semsarzadeh, M, Navarchian, A, “Effects of NCO/OH Ratio and Catalyst Concentration on Structure, Thermal Stability, and Crosslink Density of Poly (Urethane-Isocyanurate).” *J. Appl. Polym. Sci.*, **90** (4) 963–972 (2003)
  58. Shamsi, R, Abdouss, M, Sadeghi, GMM, Taromi, FA, “Synthesis and Characterization of Novel Polyurethanes Based on Aminolysis of Poly (Ethylene Terephthalate) Wastes, and Evaluation of Their Thermal and Mechanical Properties.” *Polym. Int.*, **58** (1) 22–30 (2009)
  59. Pegoretti, A, Dorigato, A, Brugnara, M, Penati, A, “Contact angle Measurements as a Tool to Investigate the Filler-Matrix Interactions in Polyurethane-Clay Nanocomposites from Blocked Prepolymer.” *Eur. Polym. J.*, **44** (6) 1662–1672 (2008)
  60. Momen, G, Farzaneh, M, “Survey of Micro/Nano Filler Use to Improve Silicone Rubber for Outdoor Insulators.” *Rev. Adv. Mater. Sci.*, **27** (1) 1–13 (2011)
  61. Eshaghi, A, Aghaei, AA, “Transparent Hydrophobic Micro-Nano Silica-Silica Nano-Composite Thin Film with Environmental Durability.” *Mater. Chem. Phys.*, **227** 318–323 (2019)
  62. Hejazi, I, Seyfi, J, Sadeghi, GMM, Jafari, SH, Khonakdar, HA, Drechsler, A, Davachi, SM, “Investigating the Interrelationship of Superhydrophobicity with Surface Morphology, Topography and Chemical Composition in Spray-Coated Polyurethane/Silica Nanocomposites.” *Polymer*, **128** 108–118 (2017)
  63. Villegas, M, Zhang, Y, Abu Jarad, N, Soleymani, L, Didar, TF, “Liquid-Infused Surfaces: A Review of Theory, Design, and Applications.” *ACS Nano*, **13** (8) 8517–8536 (2019)
  64. Verma, G, Kaushik, A, Ghosh, AK, “Nano-Interfaces Between Clay Platelets and Polyurethane Hard Segments in Spray Coated Automotive Nanocomposites.” *Prog. Org. Coat.*, **99** 282–294 (2016)
  65. Przybyszewski, B, Boczkowska, A, Kozera, R, Mora, J, Garcia, P, Aguero, A, Borrás, A, “Hydrophobic and Icephobic Behaviour of Polyurethane-Based Nanocomposite Coatings.” *Coatings*, **9** (12) 811 (2019)

66. Simpson, JT, Hunte, SR, Aytug, T, “Superhydrophobic Materials and Coatings: A Review.” *Rep. Progr. Phys.*, **78** (8) 086501 (2015)

Springer Nature or its licensor (e.g. a society or other partner) holds exclusive rights to this article under a publishing agreement with the author(s) or other rightsholder(s); author self-archiving of the accepted manuscript version of this article is solely governed by the terms of such publishing agreement and applicable law.

**Publisher's Note** Springer Nature remains neutral with regard to jurisdictional claims in published maps and institutional affiliations.